Honors Research Projects

The Dr. Gary B. and Pamela S. Williams Honors College

Spring 2017

Effects of novel fragment-warhead adducts in situ and in vitro with glutaredoxin orthologs.

Andrew J. Caras
The University of Akron, ajc127@zips.uakron.edu

Effects of novel fragment-warhead adducts *in situ* and *in vitro* with glutaredoxin orthologs.

Andrew J. Caras

Department of Chemistry

Honors Research Project

Submitted to

The Honors College

Honors Research Project

1. Abstract

Fragment-based drug design (FBDD) is a method of pharmaceutical research involving characterization of small "fragment" molecule interactions with a target protein. These fragments are optimized with the addition of a nucleophilic "warhead" moiety. Several novel fragment-warhead adducts have been synthesized *in house* by group member Ram Khattri Ph.D. The experiment investigates reactivity of these adducts with glutaredoxin protein (Grx) orthologs from *Homo sapiens*, *Pseudomonas aeruginosa* and *Brucella melitensis*. Three novel fragment-warhead adducts have been identified to cause weakly bacteriostatic and bacteriocidal effects, most with minimum inhibitory concentration values near 1.28 mg/mL. Discussed herein are molecular effects of these fragment-warhead compounds on Grx, such as their association in inducing Grx oligomerization. Further investigation of the fragment-warhead adduct coumarin acrylamide was performed due to its fluorescent properties. Use of Grx as a druggable candidate for development of a putative antibiotic has been a relatively untapped target until recently. These results may help further characterize Grx, and its ability to mediate bacterial survivability, to aid in the fight against multi-drug resistant and opportunistic bacterial infections such as pneumonia and brucellosis.

2. Introduction

Glutaredoxin (Grx) is a small (≈10 kDa) enzyme of about 100 amino acid residues that associates with a glutathione (GSH) cofactor. It is related in function to thioredoxins, a small class of redox enzymes.[1] The primary role of Grx, as investigated in mammals, is to facilitate the reversible process of protein glutathionylation and deglutathionylation[2]. The glutathionylation reaction involves the reversible conjugation of GSH to a target protein active site (usually containing a Cys residue), which modulates target protein structure and function.[3,4]

Deglutathionylation has been identified as a ping-pong reaction: Grx transfers a glutathionyl (GS) molecule from a target protein (protein-SSG) to itself (to form Grx-SSG); in the second half of the reaction, reduced glutathione (GSH) reacts with Grx-SSG to form reduced Grx (Grx-SH) and oxidized glutathione (GSSG).[2,5] Some proto-oncogenic proteins involved in apoptotic signaling have been found to depend on glutathionylation, suggesting that Grx activity is important to cancer development.[3] Grx and thioredoxins (Trx) are also involved in deoxyribonucleotide synthesis by regenerating ribonucleotide reductase which becomes oxidized during conversion of ribose to deoxyribose.[6] Previous investigations support that Trx are involved in the reduction of reactive oxygen species (ROS), which in abundance can cause cell toxicity.[7] Grx has been shown to be involved in the same process.[8]

Recently, Grx has been suggested as a drug target in various inflammatory diseases and opportunistic infections. *Pseudomonas aeruginosa*, a Gram-negative aerobic bacterium, is an increasingly common cause of hospital-acquired pneumonia that responds poorly to modern antibiotics.[3] The low antibiotic susceptibility of *P. aeruginosa* is attributed to efflux-mediated multiresistance of antibacterial compounds and a high degree of horizontal gene transfer.[9] This organism's propensity to form biofilms has also complicated treatment of infected individuals.[10,11] Combined, these traits have caused an increase in multi-drug resistant (MDR) pneumonia infections. Patients with cystic fibrosis are especially vulnerable to these infections.[12] It is evident that discovery of a new method to incapacitate *P. aeruginosa* is required. Grx has been suggested as a novel drug target due to ROS accumulation following its inhibition and possible perturbation of the glutathionylation/deglutathionylation pathway.[3,13] Grx's role in inflammatory conditions, such as tobacco smoking-induced emphysema, has also been suggested to be important in pathophysiology of these diseases.[3,14–16]

Infection by *Brucella* spp. results in brucellosis, the most common zoonotic infection worldwide.[17,18] Prevalence rates of brucellosis are greater than 10 per 100,000 citizens in some countries, a likely underreported statistic.[19] Although risk of mortality is relatively low (5%), genitourinary and hematological complications are common.[18] Eastern European, Middle-Eastern, and Asian countries have the highest rates of brucellosis. However, Mexico, and even the states of Hawaii and Texas in the United States, are purported to contain elusive harbors for brucellosis.[19] Attention should be focused on discovering a more effective treatment for brucellosis, as it often requires a cocktail of drugs for adequate treatment.[18] Differences in *B. melitensis* Grx structure near the active site, compared to other orthologs, suggests the presence of a potential selective antibiotic target in *Brucella* spp.[20]

The project focuses on investigation of novel fragment-warhead compounds. These compounds have been synthesized *in-house* by my graduate supervisor, Ram Khattri Ph.D., by screening a 463-member library of organic chemical fragments (Maybridge and Fisher). These fragments are small organic molecules that abide by the

Figure 1. Structure of RK088 ACP, an example of a fragment-warhead adduct. The driving group fragment, RK088, is shown within the dashed circle. The acryloyl moiety (warhead) is shown within the solid-line box. The nitrogen involved in the amide bond is derived from the driving group.

"rule of three" commonly used in FBDD: molecular weight < 300, number of hydrogen bond donors/acceptors < 3, and a ClogP value < 3.[21] Several fragments have been identified via ^{15}N heteronuclear single quantum coherence (HSQC) NMR spectroscopy as conferring specificity for glutaredoxin orthologs, and even within the orthologs.[22] These fragments are called "driving groups," and are somewhat hydrophobic to allow for passage through the cell membrane.

Optimization of "driving group" fragments is performed by covalently binding to it a small electrophilic moiety called a "warhead" (**Fig. 1**). Various fragment-warhead chemical adducts have been synthesized by Dr. Khattri. Compounds previously synthesized have been investigated by past members of Dr. Leeper's group.[23]
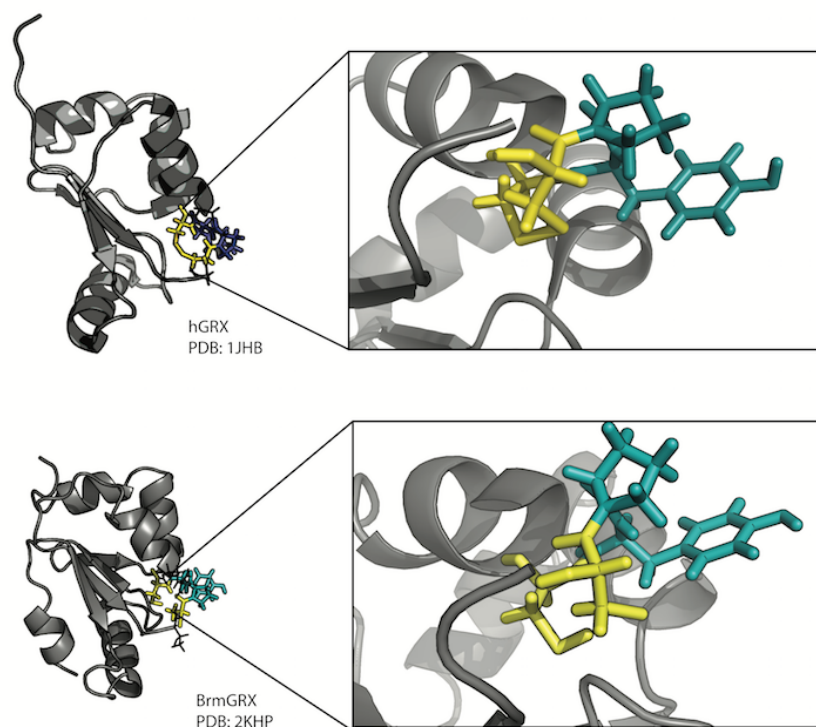
Figure 2. Solution structures of hGRX1 (PDB: 1JHB)[29] and BrmGRX (PDB: 2KHP)[20], with the CPYC active-site motif magnified. Cys residues are in yellow. Created with The PyMOL Molecular Graphics System, Version 1.3, Schrödinger, LLC.

Grx orthologs investigated herein contain an active site characterized by the "CYPC" motif. The two Cys residues are critically important to the physiological function of Grx and its ability to mediate intracellular redox state. The Tyr residue maintains an optimal enzymatic environment; mutagenesis of Tyr lowers the pKa of the N-terminal active site Cys residue.[24] The lowered pKa potentially creates a nucleophilic Cys thiolate that may have increased reactivity towards electrophilic acrylamide and acrylate moieties in comparison to the Cys thiol in wild-type Grx.

Many of the warheads contain an electrophilic vinyl group. The goal is to covalently bind the fragment-warhead compound, using this vinyl group, to the nucleophilic thiol moiety on Cys residues in the active site. A thioether between the drug and the protein is presumed to result from this Michael reaction. It is hypothesized that binding of Grx active-site Cys residue to the fragment-warhead compound will inhibit function of the enzyme and therefore lead to target organism death by increased intracellular levels of ROS. The Michael addition is hypothesized to occur readily at physiological conditions and selectively for thiolate groups on amino acid residues, further rationalizing a focus towards modulation of cysteine chemistry in drug design.[25]

It was observed that coumarin acrylamide ("coumarin AA") retained its fluorescence upon excitation with long-wavelength UV light and traveled through acrylamide gels used in SDS-PAGE; therefore, properties of this compound were further investigated. It is hypothesized that coumarin AA may interact with BrmGRX, possibly covalently with Cys residues in the active site via a Michael reaction. The results observed in SDS-PAGE were unexpected; ^{15}N heteronuclear single quantum coherence (HSQC) NMR spectroscopy performed by Khattri displayed a low degree of covalent binding of coumarin AA to BrmGRX.[22]

Effects upon incubation of novel fragment-warhead complexes with three Grx orthologs will be discussed: PaGRX (*Pseudomonas aeruginosa*); BrmGRX (*Brucella melitensis*); and hGRX1 (*Homo sapiens*). Investigation of PaGRX and BrmGRX was performed due to the purported importance of Grx in proliferation of these bacterial species. The human ortholog was included to determine if a putative fragment-warhead compound interacts selectively to a bacterial ortholog without undesirably interacting with the human ortholog. The goal of the work is to further identify reactivity of these fragment-warhead complexes towards Grx orthologs, as well as to determine bacteriocidal and bacteriostatic efficacy of these complexes.

3. Materials and Methods

Recipes for media and buffers used throughout these experiments are presented in Appendix B.

Bacterial transformation

Transformation of competent *E. coli* BL21(DE3) cells was required for PaGRX expression. Cells were thawed and incubated on ice for 15 minutes with 1 μL of 50 ng/mL PaGRX plasmid. To induce incorporation of the plasmid, the solution was then heat shocked by placing the cryovial in a 42°C water bath for 30 seconds, after which the solution was incubated on ice for 2 minutes. Heat shocking induces stress in the cell. As a result, the cell opens molecular pores to try to gain DNA from the environment that could possibly help it overcome the stressful situation. The BL21 (DE3) strain contains a high intracellular concentration of divalent cations, resulting in abundant opening of molecular pores when the cell is stressed and more robust plasmid incorporation into the host genome. To the cryovial was then added 0.5 mL of SOC media, prewarmed to 37°C. The solution was placed in an incubated shaker for 30 minutes at 37°C and 200 rpm.

Two Petri dishes were prepared by pouring LB media supplemented with 0.1 mg/mL kanamycin. Because the plates were kept in the refrigerator, they were prewarmed at 37°C. PaGRX plasmid contains a kanamycin resistance gene; therefore, use of this antibiotic will aid in selection of a colony of transformed cells. Because the number of transformed cells in the solution is unknown, unequal volumes of cells are plated. In this experiment, 100 μL and 400 μL aliquots of cell solution were plated onto separate Petri dishes. Sterile technique was used where appropriate (Appendix A). Plated cell solution was spread evenly using a sterilized stainless steel cell spreader. To ensure that the spreader had cooled enough to not harm the cells, the spreader was first placed

into an area of media on the plate that did not have the cell solution on it. If the spreader did not create a divot in the media, it was used to spread the cells. Plates were incubated overnight at 37°C.

Revival of glycerol cell stocks

Transformed *E. coli* BL21(DE3) had been prepared by previous group members for expression of BrmGRX and hGRX. These samples were stored in a 30% glycerol stock in liquid nitrogen. Sterile technique was used throughout the revival process. To a 10 mL culture tube was added 5 mL of LB media, supplemented with 0.1 mg/mL kanamycin (for hGRX) or 0.025 mg/mL carbenicillin (for BrmGRX). Media was incubated at 37°C. Using an inoculation loop, several swipes were made on the top of the slightly thawed glycerol cell stock and the loop was placed into the media. Cell solution was placed overnight in a shaking incubator at 37°C and 260 rpm.

Two plates, each containing LB media and 0.1 mg/mL kanamycin (for hGRX) or 0.025 mg/mL carbenicillin (for BrmGRX), were prewarmed the next day at 37°C. To these plates was added either 100 µL or 400 µL of the cell inoculum, which had become turbid. Plates were incubated overnight at 37°C.

Heterologous expression

Isolated colonies were picked using an inoculation loop and placed in 25 mL of M9 media (Appendix B), supplemented with the proper antibiotic for the Grx ortholog expressed, prewarmed at 37°C in a 200 mL Fernbach flask. This small-scale inoculation was kept overnight in a shaking incubator at 37°C and 260 rpm. A 20 mL aliquot of the small-scale inoculation was then added to 450 mL of the same media, prewarmed at 37°C in a 2600 mL Fernbach flask. This large-scale inoculation was placed in a shaking incubator at 37°C and 260 rpm. Cell growth was measured

using optical density at 600 nm (OD_{600}). A small aliquot of cell-free media was retained in a cuvette

to be used as a blank. Cell solution was measured every half hour. When the OD_{600} reached ≥ 0.6

Abs units, indicating peak log growth, isopropyl β-D-1-thiogalactopyranoside (IPTG) was added

to the solution to yield a concentration of 0.5 mM. The Grx plasmids were inserted into the *lac*

operon. IPTG, a lactose metabolite, promoted expression of the *lac* operon and therefore provided

an optimal environment for heterologous expression of Grx. Temperature in the shaking incubator

was dropped to 18°C for PaGRX expression; prior experimentation has found that BL21(DE3)

cells express PaGRX best at this temperature (Dan Morris; unpublished data). Cell solution was

incubated in a shaker overnight at 18°C and 260 rpm. For hGRX and BrmGRX expression, the

incubator was maintained at 37°C and 260 rpm overnight.

Extraction and purification of Grx

The cell suspension was centrifuged at 8000 x *g* for 10 minutes at 4°C; supernatant was

discarded. The cell pellet was resuspended in 25 mL of Buffer A (Appendix B), supplemented

with 10 μM each of leupeptin, benzamide and PMSF to inhibit protease activity. Cells were lysed

with a French pressure cell and then centrifuged at 14,000 x *g* for 10 minutes at 4°C. A small

aliquot of cell pellet and lysed supernatant was retained for protein purification analysis.

Supernatant was filtered using a 0.2 μm GD/X syringe filter (GE Healthcare Life Sciences) to

remove cellular debris from the sample.

Supernatant was purified using immobilized metal ion affinity chromatography (IMAC).

For maximum efficiency, an AKTA fast-performance liquid chromatography (FPLC) system was

used (GE Healthcare Life Sciences). A 5 mL HisTrap HP column was used, with the stationary

phase consisting of Ni-Sepharose (GE Healthcare Life Sciences). For some samples with a high

amount of suspected Grx expression, two HisTrap HP columns were used in series to increase the effective length of the column and purification efficacy. A two-buffer system was used for the mobile phase (Appendix B). The column was equilibrated with 5 volume-equivalents (25 mL) of Buffer A, then Buffer B, then Buffer A. Protein sample, typically ≈ 30 mL, was loaded into a 50 mL Superloop™ (GE Healthcare Life Sciences) and injected into the HisTrap column using Buffer A. Buffer B was injected over two minutes in a 0-100% gradient, to elute protein from the column. Both buffers contained 2 mM of dithiothreitol (DTT) to provide a reducing environment for protein and limit aggregation. All recombinant Grx proteins that were purified incorporate an N-terminal 6-His tag, which selectively allows Grx to bind to the Ni-Sepharose column. Buffer B contains a high concentration of imidazole; this mimics the structure of His, and in high concentrations (such as in Buffer B) competes with His and elutes the protein from the column. Fractions with high absorbance at 280 nm after eluting with Buffer B were retained and placed in SnakeSkin™ 3.5 kDa molecular weight cut-off (MWCO) dialysis tubing (ThermoFisher). A site-selective protease was added to the sample to cleave the 6-His tag. For PaGRX and hGRX, this protease was tobacco etch virus (TEV) that was prepared *in-house*. For BrmGRX, Pierce™ HRV 3C protease (ThermoFisher) was used. The sample was dialyzed overnight at 4°C in 2 L of Buffer A, then purified using the AKTA FPLC system in a similar manner as before. The eluent when using Buffer A was retained, as this sample contains protein without the 6-His tag. Eluent from Buffer B was also retained; either TEV protease or HRV 3C protease was added and the sample was dialyzed and purified as mentioned. Buffer exchange (from Tris-Cl to Na-Phos) was performed on the 6-His-cleaved sample by dialyzing for two days at 4°C in 2 L of 40 mM Na-Phos pH 7.0, 150 mM NaCl, and 2 mM DTT.

The 6-His-cleaved sample was concentrated using a 10 mL Amicon stirred cell (Millipore) and a 3.5 kDa MWCO membrane in a pressurized hypoxic environment ($\approx$60 psi of N_2) to limit protein oxidation and expedite concentration. Aromatic amino acid residues exhibit strong absorbance at 280 nm. Therefore, to monitor protein concentration, absorbance at 280 nm (A_{280}) of sample within the stirred cell was measured periodically. Flow-through from the stirred cell was used to blank the spectrophotometer (Genesys 6, ThermoFisher). A 20-fold dilution of concentrated protein was added to the cuvette (35 µL of concentrated protein in 665 µL of flow through). Extinction coefficients for the three Grx orthologs investigated can be seen in Appendix C. Concentration was completed when [Grx] $\approx$ 0.6 mM. The sample was aliquoted into 1.5 mL cryovials and stored in liquid nitrogen. Typical yields for each ortholog averaged about 24 mg (BrmGRX), 5 mg (PaGRX) and 5 mg (hGRX) from each liter of growth culture.

SDS-PAGE (protein purification)

For each protein purification, sodium dodecyl sulfate-polyacrylamide gel electrophoresis (SDS-PAGE) was performed to determine if molecular weight of the protein sample matched that of Grx. It was also used to determine degree of Grx expression in relation to other proteins in the cell and purity of Grx in the final sample. An 18% acrylamide 10-well precast gel was used (Bio-Rad). A PageRuler™ ladder (ThermoFisher) was used; 5 µL of this ladder was loaded into one of the wells. A 10 µL aliquot of each sample was added to 10 µL of 2X loading buffer (Appendix B). For all samples, 10 µL of loading buffer/sample mixture was loaded into each well. Electrophoresis buffer was a Tris-Gly-SDS mixture (Appendix B). Gel was run at 200 V for 30 minutes, or until the dye front reached about 2 cm from the end of the gel, and was stained using Coomassie Blue

G-250 stain solution (Appendix B) to observe the protein bands. Gel was placed on a rocking stand for 48-72 hours, then destained using Millipore-distilled H_2O.

Minimum inhibitory concentration (MIC) and minimum bacteriocidal concentration (MBC) assay

To determine concentration of fragment-warhead compounds required to inhibit bacterial growth, a minimum inhibitory concentration (MIC) assay was performed. Six compounds were tested: RK088, RK088 ACP, RK395 CAA, coumarin AA, acrylamide, and iodoacetamide (**Fig. 3**). *E. coli* and *P. aeruginosa* (PA01) were used. Because it is required that *B. melitensis* be handled using BSL-3 precautions, it was unable to be assayed using this technique[26].

E. coli and *P. aeruginosa* (PA01) cultures were incubated in 5 mL of LB media (Appendix B) at 37°C and 260 rpm overnight. Both cell cultures were then transferred to 5 mL Mueller-Hinton (MH) broth, prepared per manufacturer directions, at 37°C and 260 rpm. A 0.5 McFarland standard was created from each culture, with an $OD_{625} = 0.101$ for *E. coli* and $OD_{625} = 0.089$ for *P. aeruginosa* (PA01).[27] Each culture was plated on MH-agar plates using 100 µL of a 10^{-1} dilution of the 0.5 McFarland standard in MH broth. This was performed to determine the colony forming units (CFU's) suspended in the 0.5 McFarland standard. A suspension was created from the 0.5 McFarland standard. The 10^{-1} diluted suspension was serially diluted to prepare 10^{-2} fold, 10^{-4} fold, 10^{-5} fold, and 10^{-6} fold dilutions. From each dilution, 100 µL was taken and plated onto a MH plate and incubated overnight at 37°C.

Dilutions of compounds to be tested were prepared. To each sterile culture tube was added 1 mL of sterilized MH broth. To the first tube was added 1 mL of the 128 mg/mL drug to make a 64 mg/mL solution. From the first tube, 1 mL was taken and added to the second tube to prepare

a 32 mg/mL solution. This serial dilution was performed for 5 more tubes until final concentration of the drug was 1 mg/mL. Optical density at 625 nm (OD_{625}) was taken for each sample as a blank.

Inoculation of *E. coli* and *P. aeruginosa* (PA01) was performed by adding 100 μL of cell suspension in 0.85% saline to 9.9 mL of sterilized MH broth. Two compounds were tested against *E. coli*: RK088 and RK088 ACP. Four compounds were tested against *P. aeruginosa*: RK395 CAA, coumarin AA, iodoacetamide, and acrylamide. From the diluted cell suspension, 200 μL was added to each of the seven drug solutions. A sterility (negative) control was prepared that only contained MH broth. A growth (positive) control was prepared that only contained the saline cell suspension dilution. The cell-drug suspension was placed in a shaking incubator overnight at 37°C and 260 rpm. Quantitatively, the MIC was defined as the concentration of drug at which OD_{625} is less than that of the positive control after overnight incubation. The MIC was also determined qualitatively by visually examining the turbidity of the solution after overnight incubation. For colored drug compounds (RK395 CAA, coumarin AA, and RK088 ACP), the OD_{625} was also determined before the addition of the bacterial cell suspension. The final OD_{625}, used to determine the MIC, was the difference between the OD_{625} measured after incubation and the OD_{625} of the drug compound at the respective concentration.

The minimum bactericidal concentration (MBC) was determined by plating the cell suspension containing the MIC of drug. Cell suspensions that contained 10^{-1} and 10^{1}-times MIC for the drug in question were also plated, for a total of three plates per drug investigated. For all plates, 100 μL of the cell + drug suspension was added; MH-agarose media was used in all plates. Plates were incubated overnight at 37°C. Colonies were counted and plates were visually inspected for growth. MBC value was determined to be the compound concentration at which no bacterial growth occurred.

Fragment-warhead time-monitored oligomerization assay

Previous experimentation performed by group member Dan Morris displayed that oligomerization is observed among Grx orthologs when some fragment-warhead compounds are added. As an initial economical tool for determining molecular effects of adding these compounds to Grx orthologs, as well as to further investigate the role of the novel compounds in inducing oligomerization, a time-monitored binding assay was performed. For each sample, a solution of 0.25 mM Grx and 1.25 mM fragment-warhead compound was prepared in 40 mM sodium phosphate buffer, pH 7.0, to make a 1:5 ratio. This ratio was used to ensure an optimal stoichiometric environment for the lead compound to interact to the Grx ortholog. All assays involved reacting a fragment-warhead compound with each Grx ortholog, unless otherwise noted. In general, 10 mL aliquots of the mixture were taken at zero hours, 3 h, 5 h, 10 h, 30 h, 50 h, 100 h and 200 h. At the time of collection for each aliquot was added 10 mL of 2x SDS-PAGE loading buffer; samples are then placed into a -20°C freezer to inhibit further progression of the reaction. Samples were kept frozen until analyzed with SDS-PAGE.
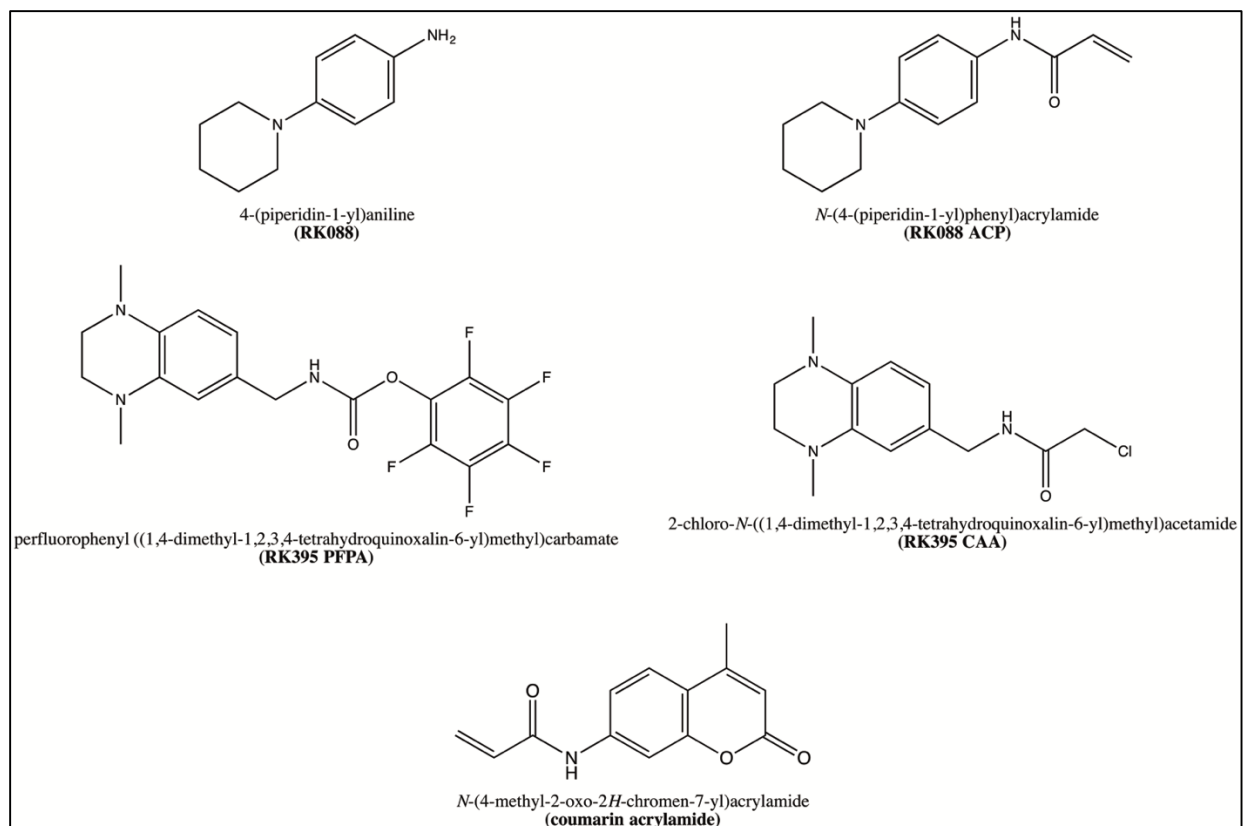
Figure 3. Structures of the fragment-warhead compounds investigated. All compounds were synthesized by Khattri. Note that RK088 is a fragment only, with no nucleophilic warhead attached. Acrylamide and iodoacetamide are not shown as individual compounds.

SDS-PAGE (drug assays)

SDS-PAGE was employed to primarily investigate degree of oligomerization, or other molecular interactions, of fragment-warhead compounds with Grx orthologs. A 4-15% acrylamide 10-well precast gradient gel was used (Bio-Rad). A PageRuler Plus™ ladder (ThermoFisher) was used; 5 µL of this ladder was loaded into one of the wells. A 10 µL aliquot of each sample was added to 10 µL of 2X loading buffer (Appendix B). For all samples, 10 µL of loading buffer/sample mixture was loaded into each well. The gel was run at 200 V for 30 minutes, or until the dye front reached about 1 cm from the end of the gel. Gel was stained using Coomassie Blue G-250 to observe protein bands by placing it on a rocking stand for 48-72 hours and then destaining using Millipore-distilled H_2O.

Thin-layer chromatography (TLC)

An attempt was made to model the chemical mechanism suggested to be involved in the biochemical interaction between BrmGRX and coumarin acrylamide. Benzyl mercaptan, a low-molecular-weight organic thiol, was employed as a model for a Cys residue. To provide an optimal stoichiometric environment for the Michael reaction to occur at room temperatures, a 5-fold excess of benzyl mercaptan (diluted in DMSO) was added to an amount of coumarin AA (diluted in DMSO) as a neat solution, and left to react for 72 hours. TLC, using silica chromatography paper, was employed to compare retention factors for coumarin AA, benzyl mercaptan, and the neat mixture. Previous experimentation by Khattri using fragment-warhead compounds has shown that an 80:20 ratio of ethyl acetate:hexane is the optimal mobile phase for maximal separation. To determine location of the non-fluorescent compounds, short UV wavelength light was shined onto the chromatography paper. Long-wavelength UV light was used to identify presence of a potential coumarin AA-benzyl mercaptan adduct, if present, as well as fluorescence of the coumarin AA control.

Investigation of benzyl mercaptan:coumarin AA:BrmGRX mixture

To further investigate the chemistry of coumarin AA, a mixture was prepared using a 5:5:1 ratio of benzyl mercaptan:coumarin AA:BrmGRX. Final concentration was 1.25 mM each for benzyl mercaptan and coumarin AA, and 0.25 mM for BrmGRX. The reaction was carried out at ambient temperature in a cryovial that was wrapped in tinfoil. The goal of this experiment was to determine if presence of benzyl mercaptan would perturb SDS-PAGE results for BrmGRX incubated with coumarin AA. Benzyl mercaptan is a Michael acceptor; therefore, it may compete with active-site Cys residues of BrmGRX for binding of coumarin AA. Samples were taken in 20

µL aliquots at the zero hour, 3 h, 5 h, 10 h, 30 h, 50 h, 100 h, 160 h, 200 h, and 400 h time points.

Samples were analyzed via SDS-PAGE.

Size exclusion chromatography

Separation of a possible coumarin AA-BrmGRX adduct was attempted using size-exclusion chromatography (SEC). A 150 µL solution containing a five-fold excess of coumarin AA to BrmGRX was prepared in a cryovial to limit exposure of the solution to air (**Table 1**). The cryovial was tightly wrapped in aluminum foil to limit light-catalyzed degradation of coumarin AA and left to react for one week at ambient temperatures. The solution was then diluted with 40 mM Na-Phos buffer, pH 7.0, to a final volume of 1 mL.

Sample	Stock	Volume	Final concentration
BrmGRX C70S	0.47 mM; in 40 mM Na-Phos, pH 7.0, with 2 mM DTT	128 µL	0.4 mM
Coumarin AA	25 mM; in DMSO	12 µL	2 mM
Na-Phos buffer, pH 7.0 (10x concentration)	400 mM	1 µL	40 mM
Millipore™ distilled H$_2$O		9 µL	
Final volume		150 µL	

Table 1. Volumes and concentrations used to prepare the 5:1 coumarinAA:BrmGRX sample. An attempt to purify this sample was performed using SEC.

Sephacryl™ S-100 high resolution (GE Healthcare) size exclusion media, stored in 20% EtOH, was used in purification of the mixture. The column was poured to 10 cm height and allowed to pack under flow. Liquid chromatography tubing was used to increase effective column length to expedite purification. Column was equilibrated with 50 mL of 40 mM Na-Phos pH 7.0. The top of the column was allowed to be very slightly exposed to air, upon which 1 mL of coumarin AA-BrmGRX solution was added directly to the top of the exposed column surface using a Pasteur

pipette. Coumarin AA-BrmGRX solution was allowed to enter the column, after which 20 mL of 40 mM Na-Phos pH 7.0 was used to elute the sample. Fluorescence of coumarin AA was used to track the band as it moved through the column, using excitation with UV light. Fractions were collected in roughly 2 mL increments; these were qualitatively measured for coumarin AA present in the sample using the UV light and determining if the solution was fluorescent. Absorbance from 240 nm to 340 nm was measured in 1 nm increments using a spectrophotometer; this range was hypothesized to detect protein present in solution, as well as the absorbance peak for coumarin AA at 328 nm. Previous studies by Khattri determined that maximum absorbance for coumarin AA (λ_{max}) was 328 nm. For a blank, 40 mM Na-Phos pH 7.0 buffer was used. A total of 10 samples were retained. Absorbance for each fraction at 280 nm and 328 nm was measured and plotted. Of the 10 fractions collected, 9 samples (fractions 2-9) were analyzed via SDS-PAGE. Apparent concentrations of BrmGRX and coumarin AA were also calculated using their respective extinction coefficients and absorbance measured at 280 nm (for BrmGRX) and 328 nm (for coumarin AA). An initial stain using Coomassie Blue G-250 solution was performed but no protein bands were seen. Due to hypothesized dilution of the protein sample, the gel was then stained using Pierce® Silver Stain for Mass Spectrometry (Thermo Scientific) following the instructions included in the kit.

4. Results

Protein purification

The primary protein purification method employed for all Grx orthologs was the use of immobilized metal ion affinity chromatography, using the AKTA FPLC system. Cell lysate is injected into the HisTrap FF column, to separate His-tagged Grx ortholog from the total sample.

Preparation of BrmGRX will be used to exemplify the results obtained for all Grx orthologs. A strong peak at 280 nm was observed in column eluent, suggestive of a high degree of BrmGRX expression (**Fig. 4**). Eluent was retained and dialyzed. The recombinant 6-His tag was cleaved using HRV 3C protease. Cleaved sample was again purified using the AKTA FPLC system and HisTrap FF column. Column flow-through, presumably containing cleaved BrmGRX, was retained (**Fig. 5**). Column eluent, presumably containing uncleaved BrmGRX, was dialyzed. 3C protease was again added to column eluent; the sample was then purified using the aforementioned methods to yield what is suggested to be cleaved BrmGRX. Samples throughout the protein purification process were collected and SDS-PAGE was performed to determine purity of the final product (**Fig. 6**).

Figure 4. Chromatogram for purification of BrmGRX cell lysate solution, using the AKTA FPLC system and the HisTrap FF column. The blue spectrum indicates absorbance at 280 nm and suggests the presence of protein. The broad first peak (between 5 and 30 mL) is the column flowthrough. The narrow second peak (fractions 3 and 4; between 65 and 75 mL) is the column eluent, likely containing BrmGRX with the recombinant 6-His tag.
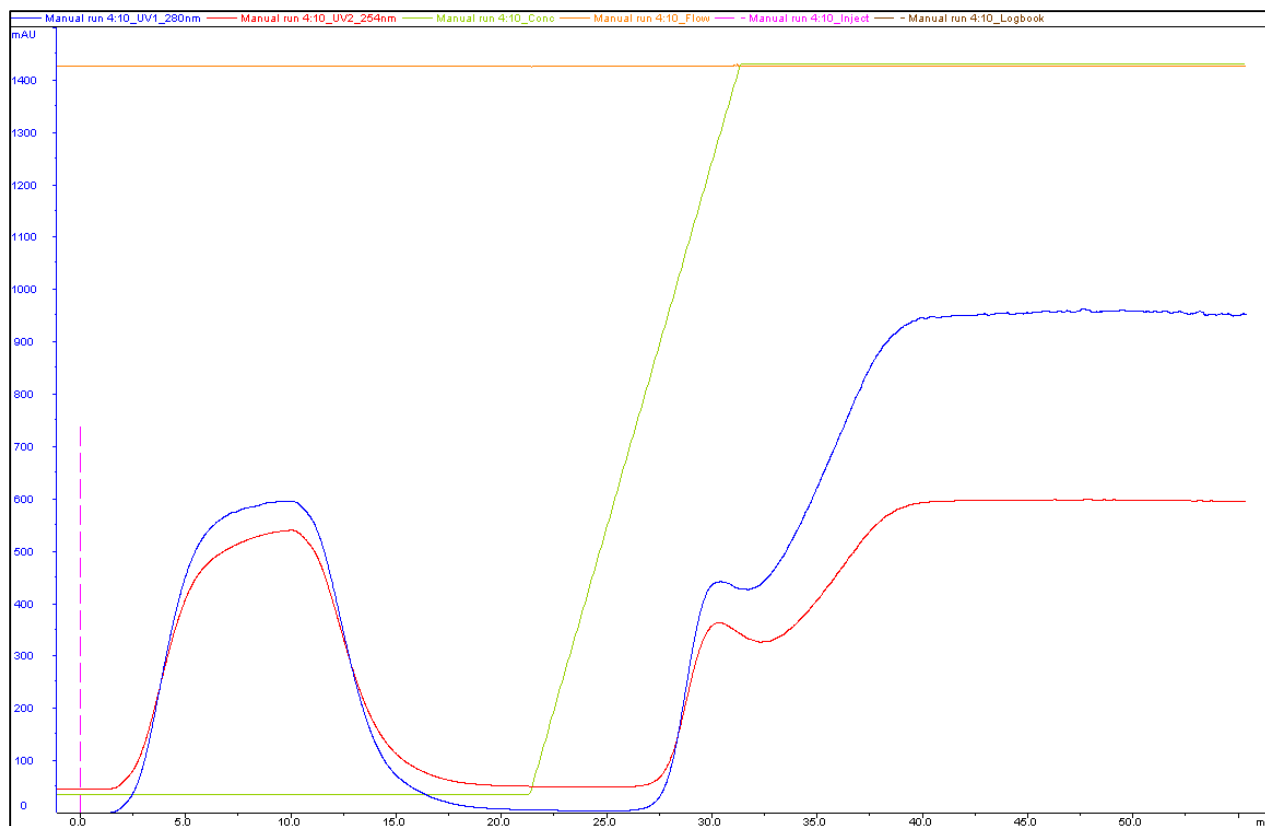
Figure 5. Chromatogram for purification of BrmGRX after cleavage of the recombinant 6-His tag, using the AKTA FPLC system and the HisTrap FF column. The blue spectrum indicates absorbance at 280 nm and suggests the presence of protein. The first peak (between 0 mL and 20 mL) is the column flowthrough and likely contains cleaved BrmGRX. The second peak (between 27.5 mL and 32.5 mL) is the column eluent; it is likely uncleaved BrmGRX (the 6-His tag is still attached). The increasing absorbance after the second elution peak, starting at 35 mL, is due to the high concentration of imidazole in the elution buffer.
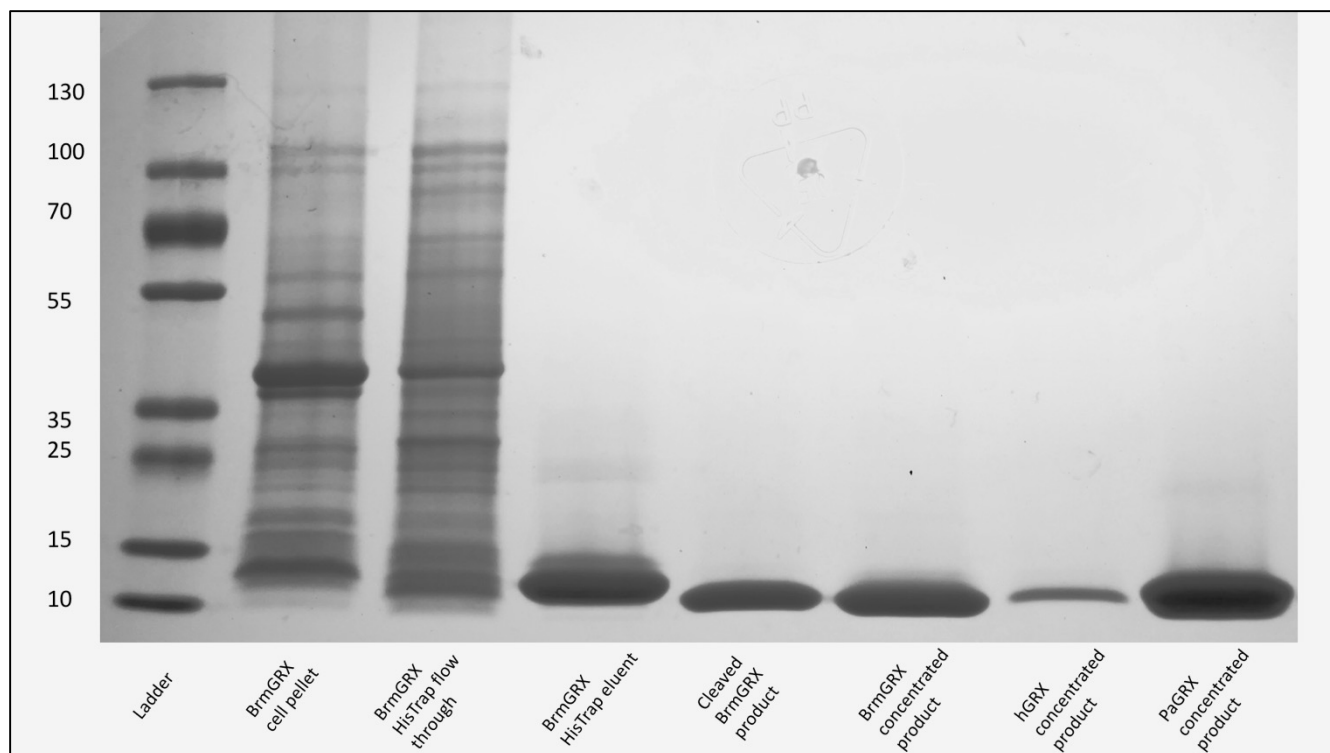
Figure 6. SDS-PAGE of various samples taken throughout the expression and purification of BrmGRX. The PageRuler Plus™ ladder is shown on the left-hand side of the image (Lane 1). Each sample is labeled on the bottom of the image. The presence of a purified final sample is suggested by a strong band between 10 and 15 kDa for the concentrated product. Samples of the concentrated product from hGRX and PaGRX expression are also displayed on this gel (lanes 7-8) to demonstrate the purity of these samples.

MIC and MBC assays

MIC and MBC assays were performed using both *E. coli* and *P. aeruginosa* upon incubation with the aforementioned fragment-warhead adducts. MIC was designated as the lowest concentration of compound added to cell culture which does not cause an increase in the OD_{625} upon 24 h of incubation (**Table 2**).

Compound	OD, 625 nm							
(mg/mL)	2.56	1.28	0.64	0.32	0.16	0.08	0.04	0
RK395 CAA	1.112	1.755	1.919	1.79	1.826	1.912	1.86	1.846
Coumarin AA	-0.021	-0.159	0.498	1.142	1.478	1.636	1.742	1.846
RK088	0.46	1.704	1.783	1.81	1.843	1.883	1.871	1.853
RK088 ACP	0.276	1.257	1.491	1.323	1.694	1.756	1.791	1.853
Acrylamide	0	1.43	1.622	1.884	1.877	1.728	1.761	1.846

Table 2. Optical density of bacterial cultures after being incubated 24 hours with the respective compound listed. Compounds were measured without bacterial culture as a blank. The OD listed for each compound is the bacterial culture OD_{625} (after adding compound) minus the OD_{625} of the compound alone in solution.

To observe fluctuation in OD_{625} among various compounds and concentrations the values were plotted, as shown in **Fig. 7**.
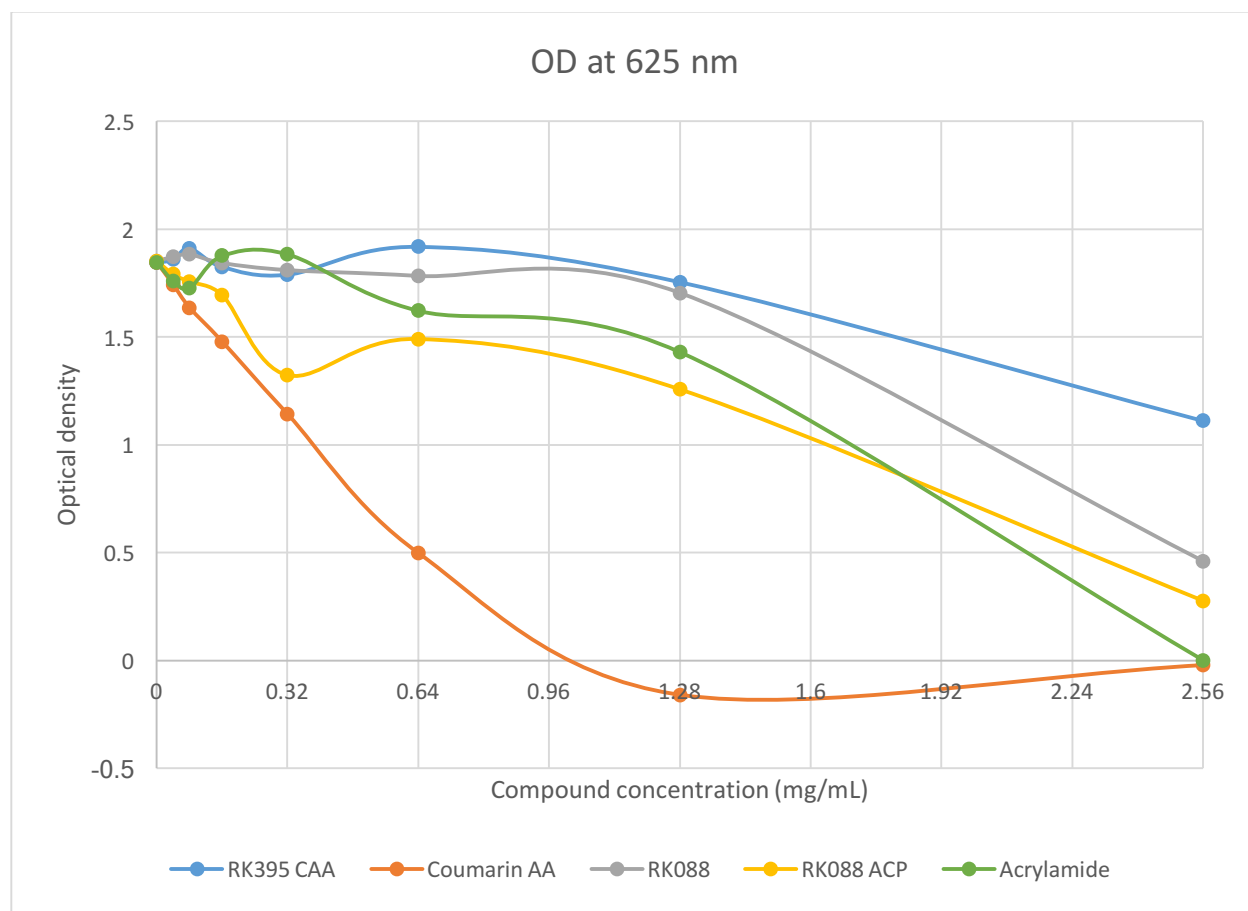
Figure 7. Plot of the optical density data in **Table 2**.

It is suggested that coumarin AA has the greatest efficacy as a bacteriostatic agent, with a MIC value between 0.08 mg/mL and 0.04 mg/mL. RK395 CAA, RK088, and RK088 ACP all have MIC values near 1.28 mg/mL. However, upon visual inspection of cultures, growth was observed near that of the positive control for cultures treated with coumarin AA (**Fig. 8**). Thus, spectrophotometric methods to determine MIC for coumarin AA are not accurate. It is possible that OD_{625} data may be perturbed by fluorescence of the compound or solubility problems of the compound in media.
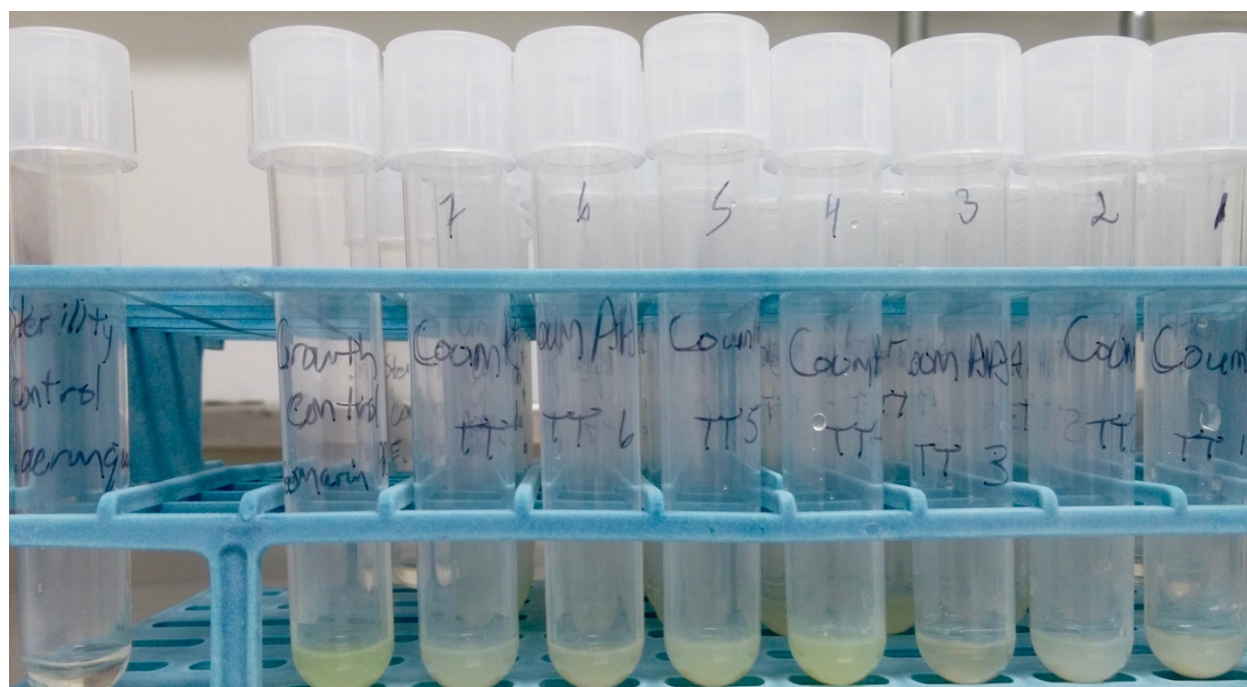
Figure 8. *P. aeruginosa* cultures incubated with various concentrations of coumarin AA (**Table 2**). It can be seen that the culture containing the highest concentration of coumarin AA (2.56 mg/mL; "TT 1," far right) became turbid in comparison to the sterility control.

MBC was determined by plating the culture containing the MIC of compound, as well as cultures with 1 unit of concentration above and below the MIC. The MBC was defined as the lowest concentration of compound which did not permit any growth of bacteria upon 24 h of incubation.
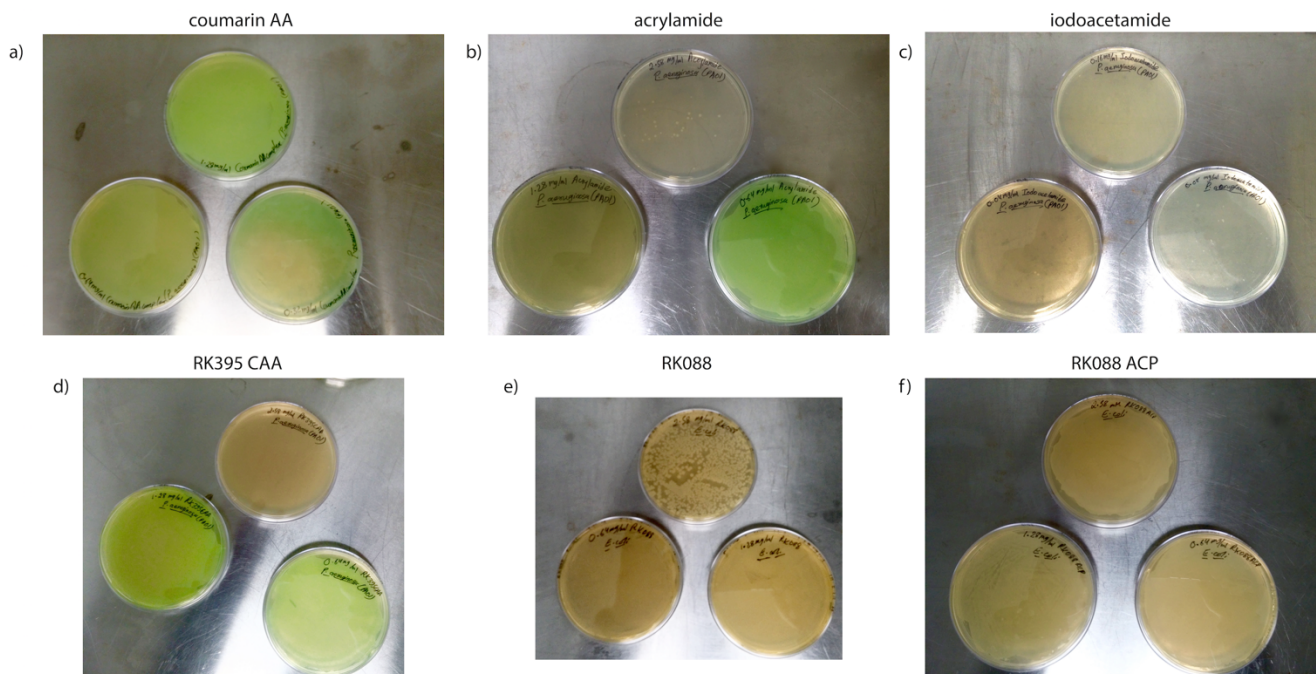
Figure 9. Images of plated *E. coli* and *P. aeruginosa* incubated with various compounds.

Coumarin AA, RK088, and RK088 ACP all have a MBC greater than 2.56 mg/mL (**Fig. 9a, e, f**). RK395 CAA has a MBC between 1.28 mg/mL and 2.56 mg/mL. The 1.28 mg/mL RK395 CAA plate displayed growth; however, the 2.56 mg/mL plate did not (**Fig. 9d**). The 2.56 mg/mL acrylamide plate displayed few colonies; therefore, the MBC for acrylamide is likely slightly above this value. Iodoacetamide displayed bacteriocidal effects at 0.04-0.08 mg/mL (**Fig. 9b**).

		Compounds					
Organism		**coumarin AA**	**acrylamide**	**iodoacetamide**	**RK395 CAA**	**RK088**	**RK088 ACP**
P. aeruginosa	**MIC (mg/mL)**	2.56	1.28	0.01	1.28		
	MBC (mg/mL)	>2.56	>2.56	0.04-0.08	1.28-2.56		
E. coli	**MIC (mg/mL)**					1.28	1.28
	MBC (mg/mL)					>2.56	>2.56

Table 3. MIC and MBC values for compounds incubated with *P. aeruginosa* and *E. coli*.

SDS-PAGE of fragment-warhead time-monitored assays

No oligomerization was observed in BrmGRX, hGRX1 or PaGRX when incubated with RK088 ACP, RK395 PFPA, or coumarin AA up to 200 hours. Oligomerization was observed in BrmGRX when given RK395 CAA, beginning at 10-hours incubation with presence of a dimer (**Fig. 10**). The dimer band increased in intensity at 30-hours incubation, with a faint trimer band. Trimer and dimer bands increased in intensity through the 200-hours incubation time point. There may be higher-order oligomers present; however, resolution of the sample at this molecular weight is too low to conclude further results.
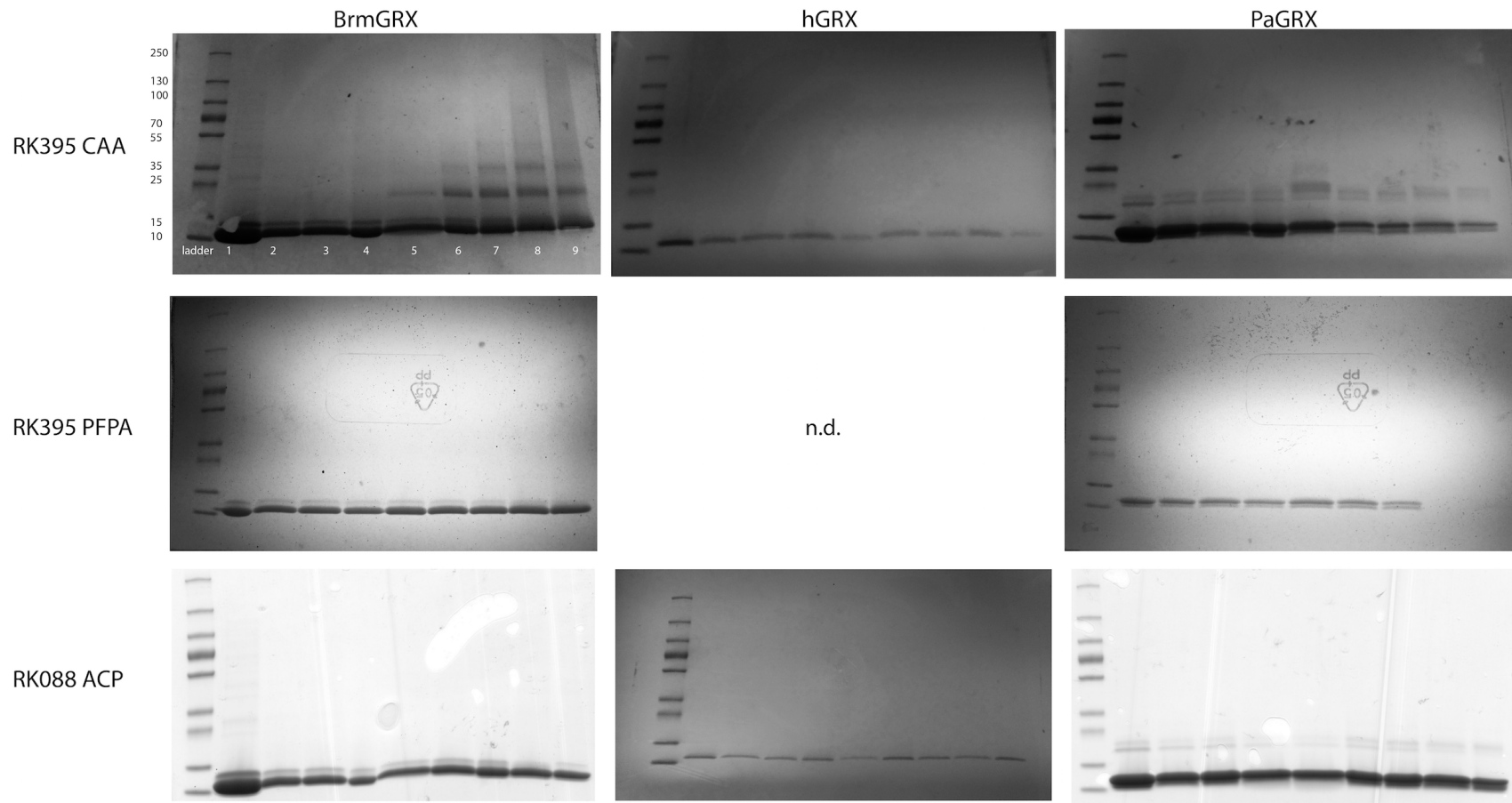
Figure 10. Images of GRX orthologs analyzed *via* SDS-PAGE after incubation with a five-fold excess of RK395 CAA, RK395 PFPA, and RK088 ACP. Oligomerization up to the trimer can be seen with BrmGRX and RK395 CAA. The ladder is marked on the first gel and is the same for all gels shown. All lanes contain the following time point samples: 1) *apo* Grx 2) zero hour 3) 3 h. incubation 4) 5 h. 5) 10 h. 6) 30 h. 7) 50 h. 8) 100 h. 9) 200 h.

Due to fluorescent properties of coumarin AA when exposed to long UV wavelengths, location of this fragment-warhead compound in the SDS-PAGE can be seen. Fluorescence of this molecule is quenched once the gel is stained with the Blue Silver colloidal dye (Coomassie Blue G-250). Incubation of coumarin AA with Grx orthologs did not cause oligomerization of Grx.
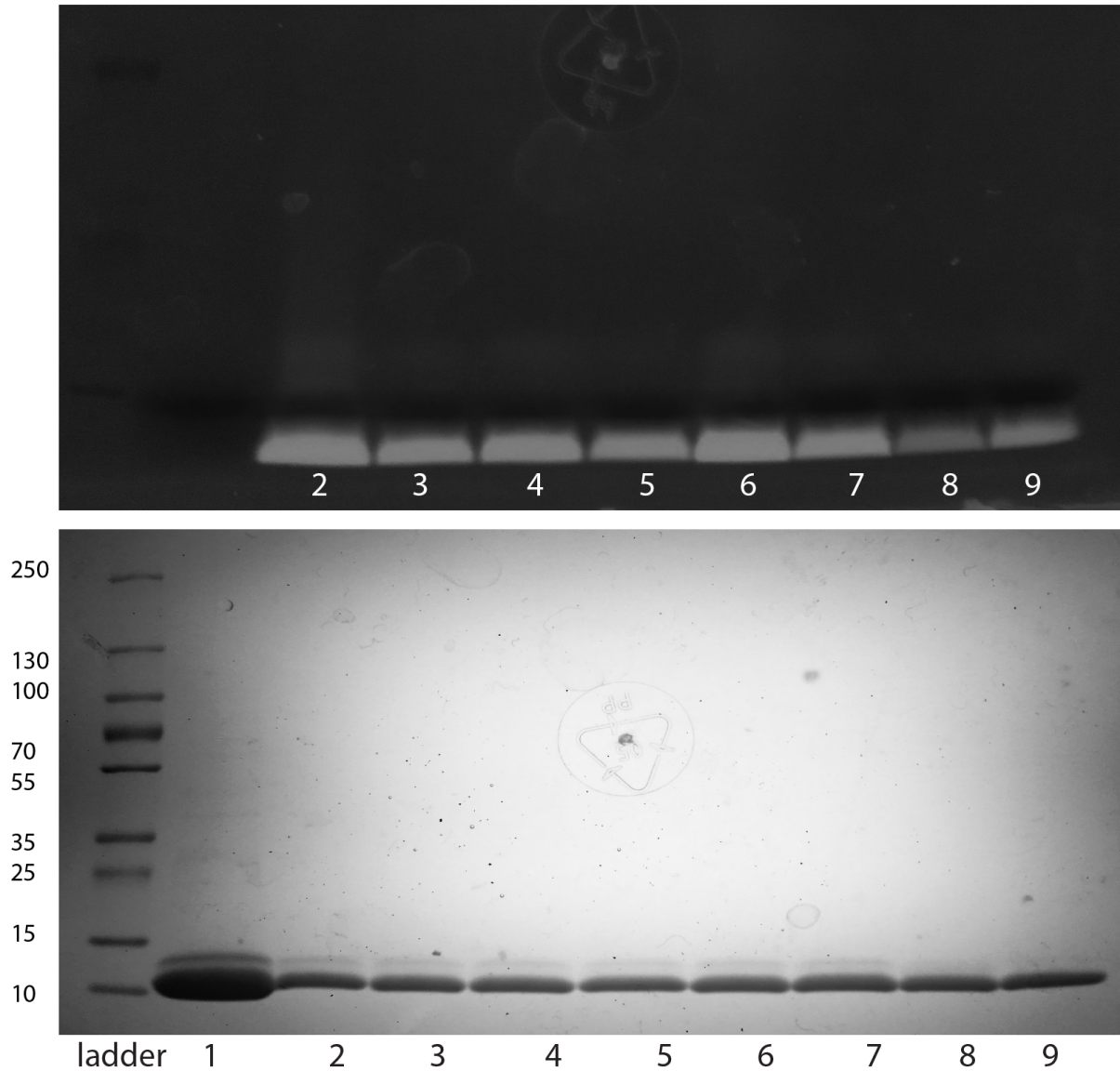
Figure 11. SDS-PAGE performed on BrmGRX samples incubated with a five-fold excess of coumarin acrylamide. The top gel was observed under long-UV wavelength fluorescence to confirm the presence of coumarin AA in the sample. The following samples were placed in each lane: 1) apo Grx 2) zero hour 3) 3 h. incubation 4) 5 h. 5) 10 h. 6) 30 h. 7) 50 h. 8) 100 h. 9) 200 h.

Thin-layer chromatography

Results from incubation of a five-fold excess of coumarin AA with benzyl mercaptan allude to the presence of a compound within the solution with a retention factor greater than that of benzyl mercaptan or coumarin AA (**Fig. 12**). Excess benzyl mercaptan can be seen on the TLC plate at the top in the third sample; however, this is expected due to its five-fold excess.
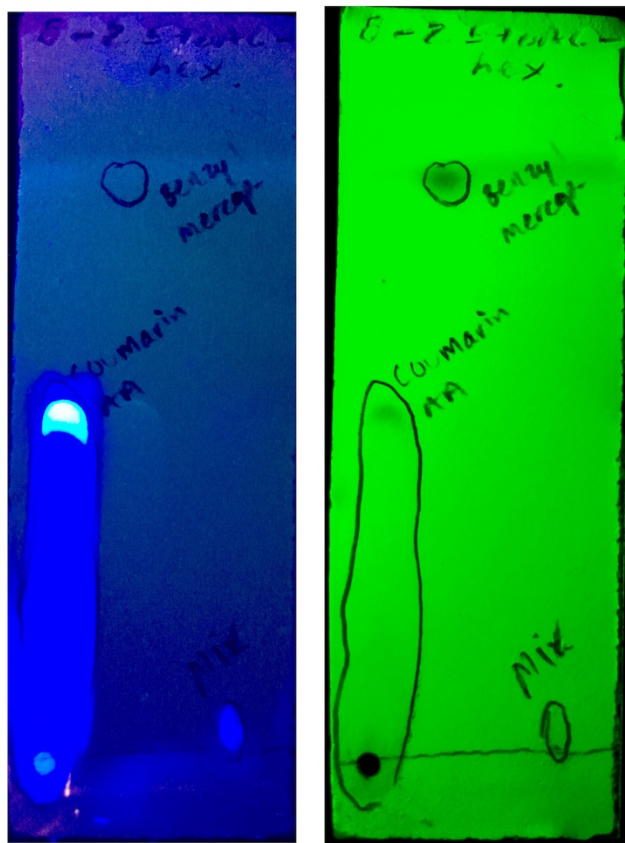
Figure 12. Silica TLC plates for the analysis of the 5:1 mixture of benzyl mercaptan:coumarin AA using an 80-20 mixture of ethyl acetate to hexane. The left-most spot was stock coumarin AA. The middle spot was benzyl mercaptan. The right-most spot was the mixture. The left TLC plate was illuminated using long-wavelength UV light to display the expected fluorescence from the coumarin AA spot, as well as potential fluorescence from the coumarin AA:benzyl mercaptan mixture. The right TLC plate was illuminated using short-wavelength UV light to better identify the position of each sample on the plate.

Investigation of benzyl mercaptan:coumarin AA:BrmGRX mixture

It was found that coumarin AA is able to travel through acrylamide gels without the presence of other molecules (such as BrmGRX). Lane 3, containing BrmGRX and coumarin AA

at 160 hours, displayed two bands between the 15 kDa ladder band and the BrmGRX band **(Fig. 13)**. Lane 6, containing BrmGRX and coumarin AA at 400 hours, displayed as a smear. This phenomenona was neither observed in samples that contained BrmGRX and benzyl mercaptan nor in samples that contained the 5:5:1 mixture of benzyl mercaptan:coumarin AA:BrmGRX.

Size exclusion chromatography

Fractions 4-10 displayed varying degrees of fluorescence when illuminated using long-UV wavelengths and inspected visually. Fraction 6 displayed the most fluorescence. The fluorescence in these fractions is inferred to be due to coumarin AA in the sample, with a higher magnitude of fluorescence indicating a higher concentration of coumarin AA in the fraction. From SDS-
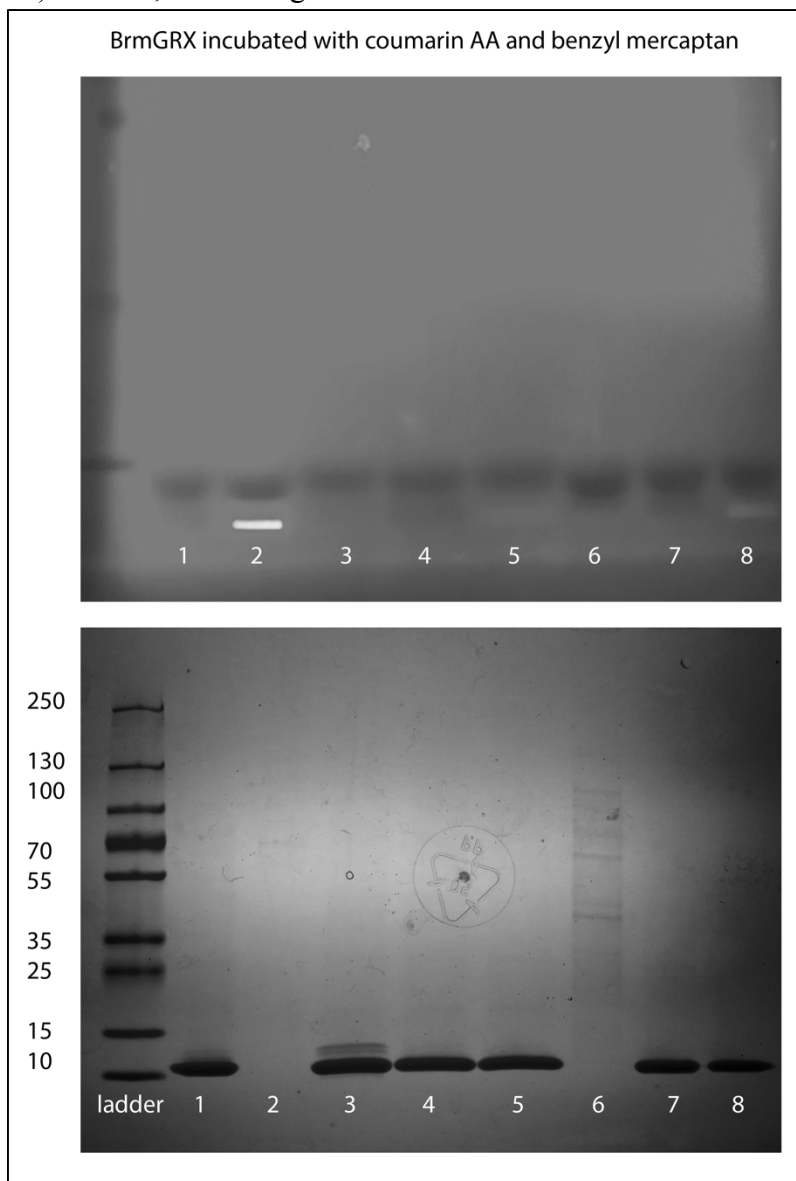
Figure 13. SDS-PAGE performed on 5:5:1 mixture of benzyl mercaptan:coumarin AA:BrmGRX. Lanes contain the following samples: 1) apo BrmGRX. 2) coumarin AA. 3) 160 h. coumarin AA+BrmGRX. 4) 160 h. benzyl mercaptan+BrmGRX. 5) 160 h. coumarin AA+benzyl mercaptan+BrmGRX. 6) 400 h. coumarin AA+BrmGRX. 7) 400 h. benzyl mercaptan+BrmGRX. 8) 400 h. coumarin AA+benzyl mercaptan+BrmGRX.

PAGE of fractions 2-10 (**Fig. 14**) it can be seen that fractions 2 through 5 contain protein between

10 and 15 kDa, presumably Grx.
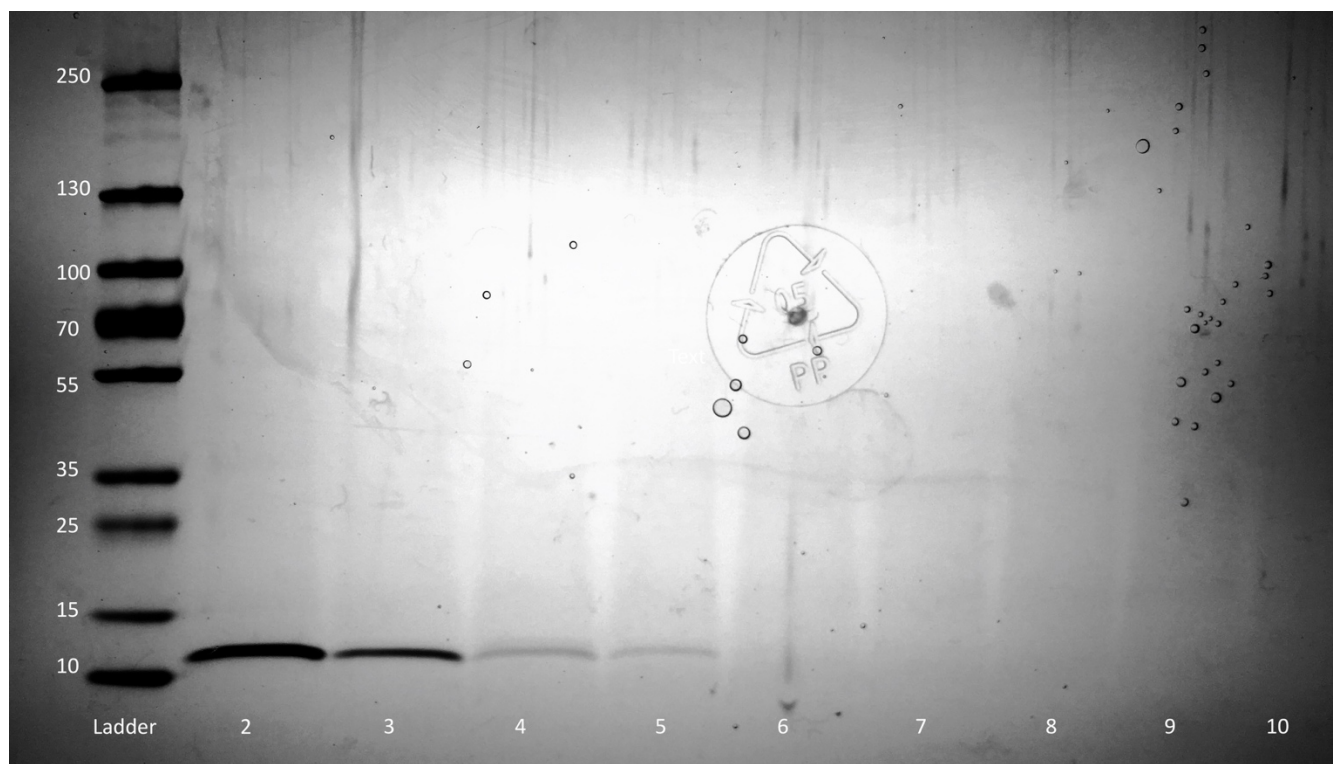
Figure 13. SDS-PAGE of Fractions 2-10 collected from size exclusion chromatography of a five-fold excess of coumarin AA incubated for 1 week with BrmGRX. A silver stain was used to show protein bands in the fractions, as significant dilution of the protein was expected to occur during SEC purification of the mixture.

SEC fractions 1-10 were also measured spectrophotometrically to measure absorbance at

280 nm (indicative of protein in solution) and 328 nm (maximal absorbance of coumarin AA, as

measured by Khattri). A plot of absorbance values at 280 nm and 328 nm was created (**Fig. 15**).

Using the extinction coefficient for coumarin acrylamide at 328 nm calculated by Khattri and the

extinction coefficient of BrmGRX (Appendix C), apparent concentrations of coumarin acrylamide

and BrmGRX in each fraction was calculated. From these calculated concentrations (**Table 3**), the

apparent ratio of BrmGRX to coumarin AA was plotted as a function of fraction number (**Fig. 16**).
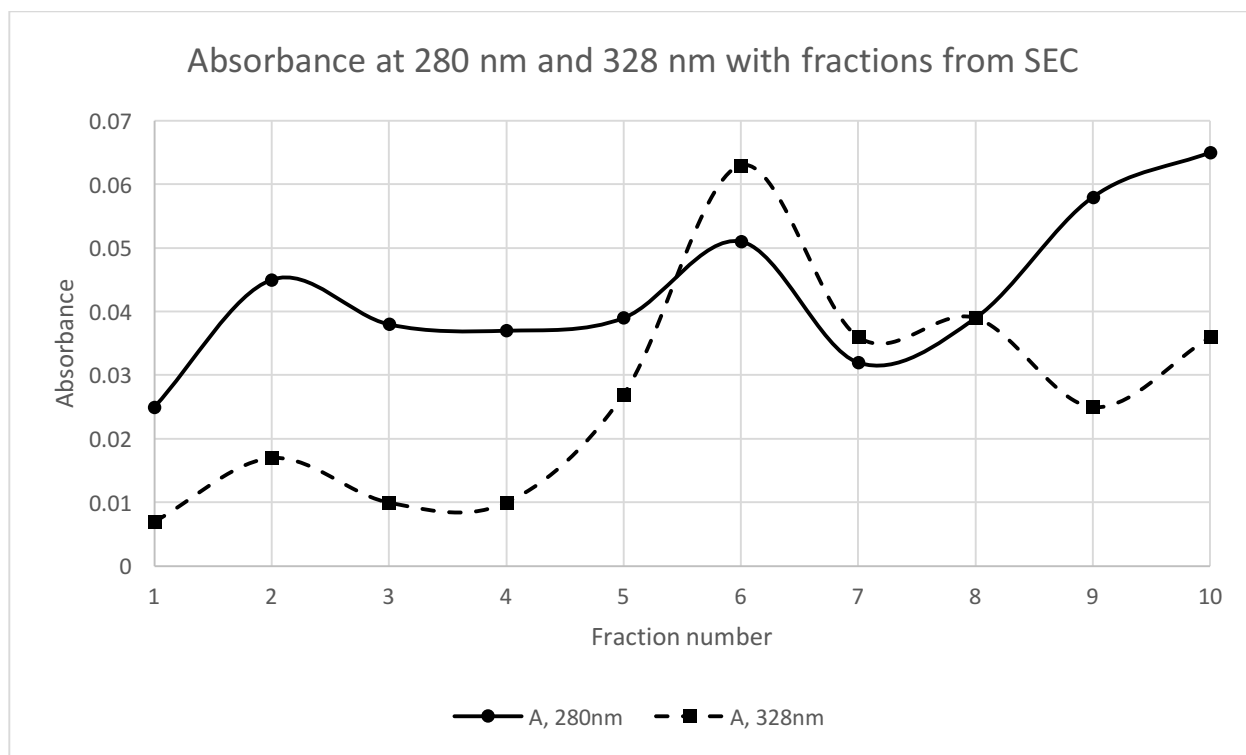
Figure 14. Absorbance at 280 nm (blue) and 328 nm (orange) for fractions 1-10.

Fraction	Calculated [BrmGRX] (µM)	Calculated [coumarin AA] (µM)
1	5.592841163	0.653167864
2	10.06711409	1.586264813
3	8.501118568	0.933096949
4	8.277404922	0.933096949
5	8.724832215	2.519361762
6	11.40939597	5.878510777
7	7.158836689	3.359149016
8	8.724832215	3.6390781
9	12.9753915	2.332742372
10	14.54138702	3.359149016

Table 4. Apparent concentrations of BrmGRX and coumarin AA in each fraction, calculated using the absorption at 280 nm (for BrmGRX) and 328 nm (for coumarin AA) and the extinction coefficient for BrmGRX and coumarin AA.
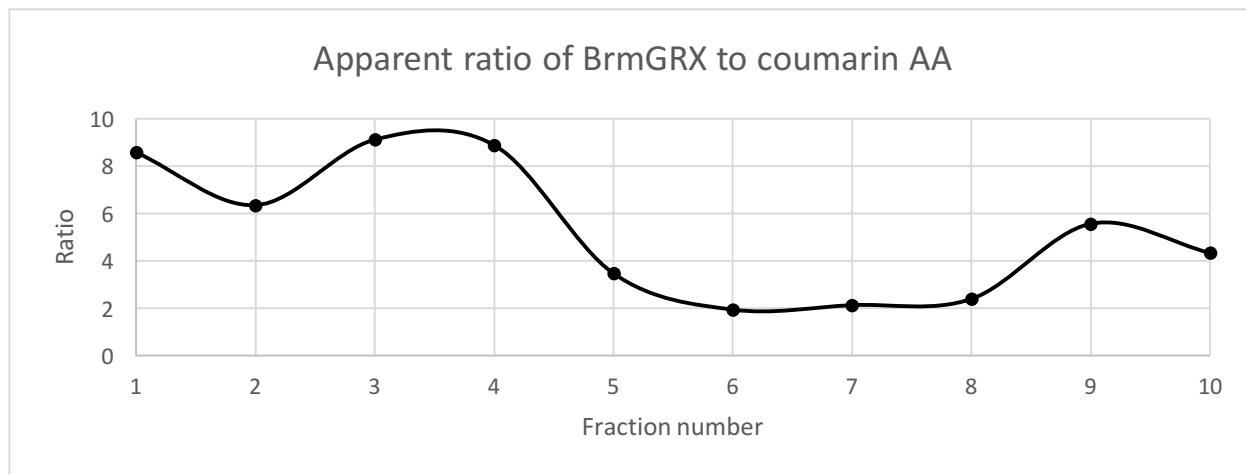
Figure 15. Apparent ratio of BrmGRX to coumarin AA in each fraction collected. The ratio for each sample was calculated by dividing the apparent concentration of BrmGRX by the apparent concentration of coumarin AA in each fraction (**Table 3**).

Calculated concentrations of BrmGRX and coumarin AA suggest that some amount of protein is present in all samples. However, SDS-PAGE (**Fig. 14**) clearly displays a lack of protein at these samples, or a concentration of protein lower than the detection limit for the silver stain used. A plot of the absorbance data (between 240 and 340 nm in 1 nm increments) was printed from the spectrophotometer (**Fig. 17**).
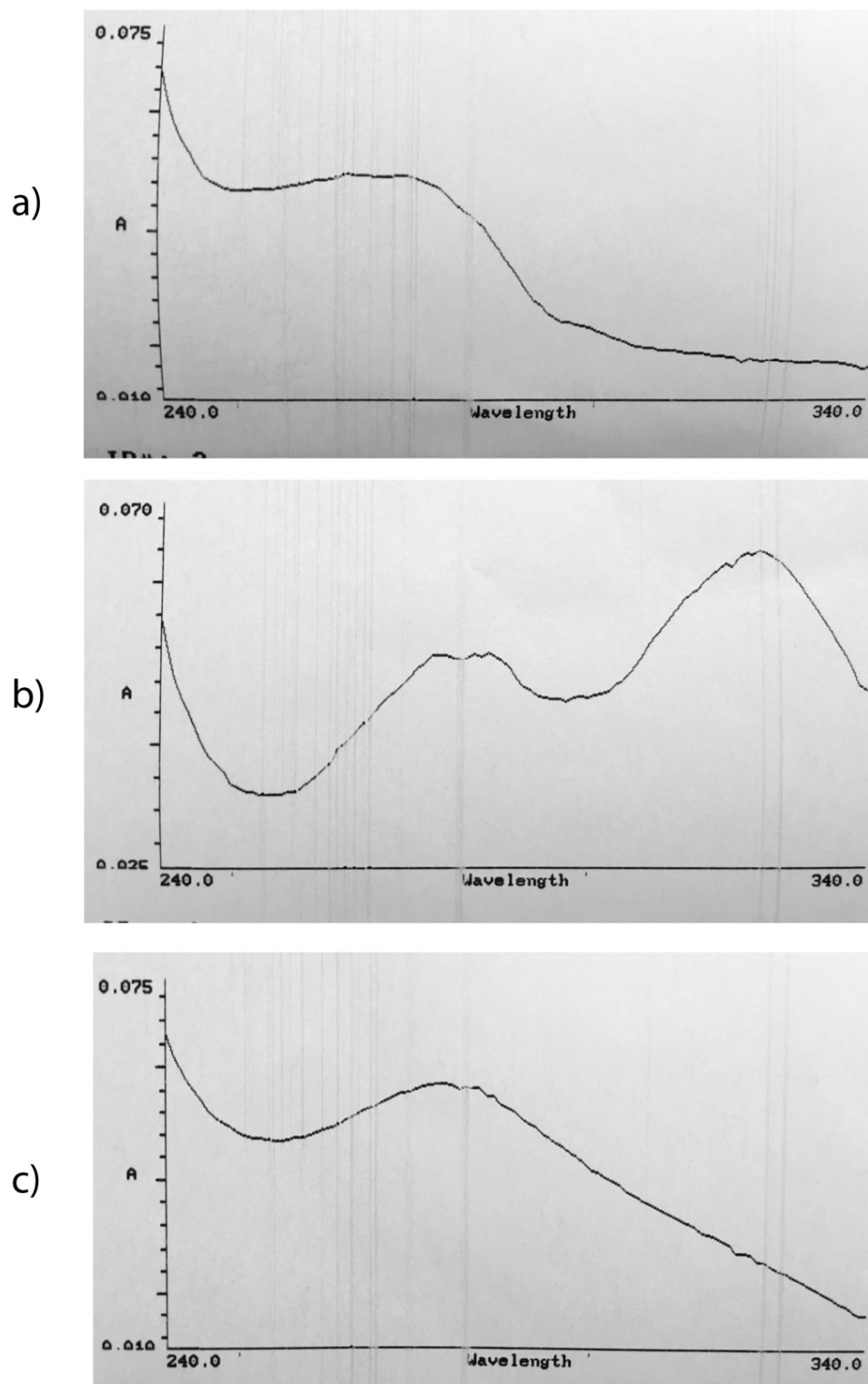
Figure 16. Examples of absorbance spectra for each of the three groups of fractions collected. a) Fraction 2, displaying a peak near 280 nm which is representative of fractions 1-5. b) Fraction 6, displaying a peak near 280 nm and a stronger peak near 330 nm which is representative of fractions 6-8. c) Fraction 9, displaying a peak near 280 nm which is representative of fractions 9 and 10.

For fractions 1-5, a single peak was seen on the plot near 280 nm, which is hypothesized to be due to protein in solution. This peak was similar in shape and position on the wavelength axis to those observed during GRX purification. Fractions 6-8 clearly displayed two peaks: one in the similar location as in fractions 1-5, and a second peak near 330 nm. The peak at 330 nm was hypothesized to result from coumarin acrylamide in the fraction, because the wavelength for maximum absorption of coumarin acrylamide (λ_{max}) was previously determined by Khattri to be 328 nm. Fractions 9 and 10 did not display a clear peak near 330 nm; instead, they displayed a peak near 280 nm and a gradual tapering in absorbance from 280 to 340 nm.

Low concentrations of Grx and coumarin AA used in this experiment warranted further investigation of the spectrophotometric properties of the buffer to determine the effect of background noise on the spectra collected. Absorbance of the buffer (40 mM Na-Phos pH 7.0) was measured from 240 nm to 340 nm using Millipore-distilled water as a blank; no absorbance peak was observed.

5. Discussion

Each Grx ortholog (PaGRX, hGRX and BrmGRX) was heterologously expressed and purified. Analysis of each sample via SDS-PAGE confirmed the identity of the purified protein as a band between 10 and 15 kDa which is indicative of Grx. MIC and MBC spectrophotometric results suggest that coumarin AA is the best bacterial inhibitor out of the fragment-warhead compounds tested; however, turbidity was observed above the MIC value indicated by the spectrum (**Fig. 7**) which indicates bacterial growth. A similar result was observed for nearly all compounds tested. It is hypothesized that poor solubility of most of these compounds in water lead to aberrant spectrophotometric results. The fragment-warhead compound RK395 CAA had the

most effective MIC value (0.64-1.28 mg/mL). Interestingly, RK395 CAA was the only fragment-warhead compound that caused oligomerization of protein, specifically BrmGRX. It is worth mentioning that RK395 CAA was tested against *P. aeruginosa* and there was no oligomerization observed in PaGRX. The potential role of fragment-warhead compounds in inducing oligomerization of Grx warrants further investigation, as it may play a role in the drug efficacy and/or bacteriostatic and bacteriocidal action. Where possible, determination of MIC and MBC of RK395 CAA when incubated with *B. melitensis* may be a worthwhile investigation.

SEC performed after incubation of BrmGRX with coumarin AA yielded contradictory results. The goal of this portion of the experiment was to attempt to identify if coumarin AA was binding to BrmGRX covalently or non-covalently. It was hypothesized that coumarin AA would travel with a strong protein band during SEC if it was a covalent binder because the environmental conditions of SEC would prevent co-elution of coumarin AA with BrmGRX in a non-covalent binding mode. Spectrophotometric results suggest a co-elution of BrmGRX and coumarin AA but SDS-PAGE results contradict this observation.

Spectrophotometric data (**Fig. 17**) suggests presence of protein, presumably BrmGRX, in samples 2, 6 and 9 as shown. Upon examination of all fractions *via* SDS-PAGE and staining with a silver stain, only fractions 2, 3, 4 and 5 showed a progressively weaker protein band. It was hypothesized that all fractions would contain some amount of protein, with fraction 6 containing the strongest protein band, due to that fraction containing the highest absorbance at 280 nm. This was not observed. With a detection limit of 0.25 ng, the silver stain is very sensitive to presence of protein. An attempt to concentrate fractions 6-10 was not performed. With the high sensitivity of the silver stain, miniscule concentrations of protein are detected; concentration would most likely not yield a different result. In **Fig. 17b**, which shows the spectrum for fraction 6, the separate

absorption peaks at 280 nm and 328 nm are clearly seen. It is hypothesized that the 280 nm peak is due to BrmGRX and that the 328 nm peak is due to coumarin AA. Further support for this hypothesis is that fraction 6 was the most fluorescent under long-wavelength UV light which suggests the presence of coumarin AA in solution.

More investigation of BrmGRX and coumarin AA is needed to further identify if coumarin AA associates covalently or non-covalently. Trypsin proteolysis may yield beneficial information. Protein bands from lanes 2-4 may be excised and treated with trypsin, a serine protease that cleaves after Lys and Arg residues except when after Pro[28]. The resulting solution can be analyzed via mass spectrometry. Trypsin proteolysis could be performed on other fractions upon further purification which could support or negate presence of protein in fractions 6 through 10. Presence or absence of covalent binding of coumarin AA would likely be seen using this experiment due to perturbed molecular weights of amino acid residues. Trypsin proteolysis could also be performed on oligomers seen upon reacting RK395 CAA with BrmGRX (**Fig. 10**). Mass spectroscopy may allude to presence or absence of fragment-warhead binding to BrmGRX in various oligomers.

6. Conclusion

Three Grx orthologs were successfully expressed in the experiment: BrmGRX (*B. melitensis*), PaGRX (*P. aeruginosa*), and hGRX (human). New fragment-warhead adducts have been tested with Grx orthologs *in situ* with *E. coli* and *P. aeruginosa* with varying degrees of success. Compound RK395 CAA was the most effective bacterial inhibitor. Compounds RK395 CAA, RK395 PFPA, and RK088 ACP were also incubated *in vitro* with BrmGRX, PaGRX and hGRX to examine molecular changes of Grx orthologs upon exposure to these compounds. Only BrmGRX when exposed to RK395 CAA exhibited oligomerization up to the trimer, suggesting

that RK395 CAA may be interacting with BrmGRX in a way to cause oligomerization. Further experimentation, such as with mass spectroscopy or a trypsin proteolysis, is required to determine how exactly this may be occurring. Characterization of Grx orthologs and fragment-warhead adducts should continue to be completed to fully probe the active site of Grx and discover a covalently-binding inhibitor of Grx. Such research can aid in the fight against multi-drug-resistant pneumonia and brucellosis.

Further investigation of coumarin AA is suggested in other Cys-trap containing proteins for its potential use as a fluorescent probe for these active sites. No definitive data have been obtained that suggests that coumarin AA binds covalently; therefore, it may be a non-covalent interaction. The hypothesis that coumarin AA interacts covalently with BrmGRX is not supported from SDS-PAGE and spectrophotometric results after SEC acquired herein. More robust experimentation is encouraged (as described earlier) to further probe interactions of this compound with Grx. If a binding mode is elucidated and it is found to be selective for Cys-trap active sites, coumarin AA could be used as an initial active site screening tool for novel or uncharacterized proteins.

Research performed herein has exposed me to biochemical techniques including protein expression, drug design, bacterial transformation and culture manipulation, gel electrophoresis, and NMR spectroscopy. I will be attending The University of Toledo College of Medicine in Fall 2017 after my undergraduate studies are completed. Knowledge obtained from these experiments will most directly benefit my understanding of pharmacology, bacterial pathophysiology, and MDR opportunistic infections. This research has also exposed me to the academic publication writing process. I also plan on performing research in medical school and as a physician. The biochemical lab skills and deeper understanding of the research process that I have acquired while

working in the Leeper group have given me the confidence and assurance that I will be able to perform such research in the future.

7. Acknowledgements

References

1.   Höög, J. O., Jörnvall, H., Holmgren, A., Carlquist, M. & Persson, M. The primary structure of Escherichia coli glutaredoxin. Distant homology with thioredoxins in a superfamily of small proteins with a redox-active cystine disulfide/cysteine dithiol. *Eur. J. Biochem.* **136,** 223–232 (1983).

2.   Gallogly, M. M., Starke, D. W. & Mieyal, J. J. Mechanistic and kinetic details of catalysis of thiol-disulfide exchange by glutaredoxins and potential mechanisms of regulation. *Antioxid. Redox Signal.* **11,** 1059–81 (2009).

3.   Ramilo, O. & Mejias, A. Glutathione on the Fas Track: A Novel Drug Target for the Treatment of Pseudomonas Infection? **189,** 386–389 (2014).

4.   Anathy, V. *et al.* Redox amplification of apoptosis by caspase-dependent cleavage of glutaredoxin 1 and S-glutathionylation of Fas. *J. Cell Biol.* **184,** 241–252 (2009).

5.   Gallogly, M. M., Starke, D. W., Leonberg, A. K., English Ospina, S. M. & Mieyal, J. J. Kinetic and mechanistic characterization and versatile catalytic properties of mammalian glutaredoxin 2: Implications for intracellular roles. *Biochemistry* **47,** 11144–11157 (2008).

6.   Fernandes, A. P. & Holmgren, A. Glutaredoxins: glutathione-dependent redox enzymes with functions far beyond a simple thioredoxin backup system. *Antioxid. Redox Signal.* **6,** 63–74 (2004).

7.   Yoshida, T., Nakamura, H., Masutani, H. & Yodoi, J. The involvement of thioredoxin and thioredoxin binding protein-2 on cellular proliferation and aging process. *Ann. N. Y. Acad. Sci.* **1055,** 1–12 (2005).

8.   Du, Y., Zhang, H., Lu, J. & Holmgren, A. Glutathione and glutaredoxin act as a backup of human thioredoxin reductase 1 to reduce thioredoxin 1 preventing cell death by aurothioglucose. *J. Biol. Chem.* **287,** 38210–38219 (2012).

9.   Poole, K. Efflux-mediated multiresistance in Gram-negative bacteria. *Clinical Microbiology and Infection* **10,** 12–26 (2004).

10.   Taylor, P. K., Yeung, A. T. Y. & Hancock, R. E. W. Antibiotic resistance in Pseudomonas aeruginosa biofilms: Towards the development of novel anti-biofilm therapies. *J. Biotechnol.* **191,** 121–130 (2014).

11.   Fothergill, J. L., Winstanley, C. & James, C. E. Novel therapeutic strategies to counter Pseudomonas aeruginosa infections. *Expert Rev. Anti. Infect. Ther.* **10,** 219–35 (2012).

12.   Khan, T. Z. *et al.* Early pulmonary inflammation in infants with cystic fibrosis. *Am. J. Respir. Crit. Care Med.* **151,** 1075–1082 (1995).

13.   Romsang, A., Leesukon, P., Duangkern, J., Vattanaviboon, P. & Mongkolsuk, S. Mutation of the gene encoding monothiol glutaredoxin (GrxD) in Pseudomonas aeruginosa increases its susceptibility to polymyxins. *Int. J. Antimicrob. Agents* **45,** 314–318 (2015).

14.   Aesif, S. W. *et al.* Ablation of glutaredoxin-1 attenuates lipopolysaccharide-induced lung inflammation and alveolar macrophage activation. *Am. J. Respir. Cell Mol. Biol.* **44,** 491–499 (2011).

15.   Kuipers, I. *et al.* Cigarette smoke targets glutaredoxin 1, increasing S-glutathionylation and epithelial cell death. *Am. J. Respir. Cell Mol. Biol.* **45,** 931–937 (2011).

16.   Chung, S., Sundar, I. K., Yao, H., Ho, Y.-S. & Rahman, I. Glutaredoxin 1 regulates cigarette smoke-mediated lung inflammation through differential modulation of I{kappa}B kinases in mice: impact on histone acetylation. *Am. J. Physiol. Lung Cell. Mol. Physiol.* **299,** L192–203 (2010).

17.   Pappas, G. The changing Brucella ecology: Novel reservoirs, new threats. *Int. J. Antimicrob. Agents* **36,** S8–S11 (2010).

18.   Franco, M. P., Mulder, M., Gilman, R. H. & Smits, H. L. Human brucellosis. *Lancet Infect. Dis.* **7,** 775–786 (2007).

19.   Pappas, G., Papadimitriou, P., Akritidis, N., Christou, L. & Tsianos, E. V. The new global map of human brucellosis. *Lancet Infect. Dis.* **6,** 91–99 (2006).

20.   Leeper, T., Zhang, S., Van Voorhis, W. C., Myler, P. J. & Varani, G. Comparative analysis of glutaredoxin domains from bacterial opportunistic pathogens. *Acta Crystallogr. Sect. F Struct. Biol. Cryst. Commun.* **67,** 1141–1147 (2011).

21.   Rees, D. C. *et al.* Fragment-Based Lead Discovery. *Nat. Rev. Drug Discov.* **3,** 660–672 (2004).

22.   Khattri, R. B. Identifying selective ligands for glutaredoxin proteins with fragment based drug design approach and optimization of the bacterial selective hits. *Ph. D. Diss. Univ. Akron Dep. Chem. Biochem. Akron, OH 44325* (2016).

23.   Napper, K. R., Morris, D. & Davis, C. Drug Interactions with Glutaredoxin Orthologues. *Honor. Res. Proj.* **Paper 173,** (2015).

24.   Foloppe, N. & Nilsson, L. The Glutaredoxin -C-P-Y-C- Motif: Influence of Peripheral Residues. *Structure* **12,** 289–300 (2004).

25.   Mather, B. D., Viswanathan, K., Miller, K. M. & Long, T. E. Michael addition reactions in macromolecular design for emerging technologies. *Prog. Polym. Sci.* **31,** 487–531 (2006).

26.   Centers for Disease Control and Prevention. Assessing Laboratory Risk Level and PEP. (2012). Available at: http://www.cdc.gov/brucellosis/laboratories/risk-level.html. (Accessed: 27th June 2016)

27.   Weinstein, M. P. *Methods for Dilution Antimicrobial Susceptibility Tests for Bacteria That Grow Aerobically; Approved Standard — Ninth Edition. Clinical and Laboratory Standards Institute.* **32,** (2012).

28.   Shevchenko, A., Tomas, H., Havlis, J., Olsen, J. V & Mann, M. In-gel digestion for mass spectrometric characterization of proteins and proteomes. *Nat. Protoc.* **1,** 2856–2860 (2006).

29.   Sun, C., Berardi, M. J. & Bushweller, J. H. The NMR solution structure of human glutaredoxin in the fully reduced form. *J. Mol. Biol.* **280,** 687–701 (1998).

Appendix A
Safety considerations.

Appendix B
Buffers and media.

Appendix C
Calculated extinction coefficients.

Appendix A. Safety considerations.

Safety glasses and nitrile gloves were worn at all times. Safety glasses blocked UV light, which was important when using UV light with coumarin AA. Nitrile gloves were mainly used to prevent contamination of the samples; however, they were also used as a last-resort barrier against acids and bases that may be used in buffer preparation. Full-length pants and fully covered shoes were worn at all times. Broken glassware was placed in the appropriate bin. Insulated gloves were used when removing or placing samples into the liquid nitrogen Dewar used for storage. Although most reagents used are relatively harmless, volatile reagents and chemicals (such as benzyl mercaptan) were worked with only in a fume hood. Care was taken to prevent unnecessary exposure to reagents. All MSDS sheets were kept in a filing cabinet in the lab. All work was supervised by a graduate member.

Sterile technique was used during bacterial transformations and plating. When working with bacterial samples, a laboratory coat was worn. The work surface was cleaned with 70% ethanol, wiped using a paper towel, and allowed to evaporate completely. Ethanol bottles were kept away from the work surface after this time. A Bunsen burner was used to create air currents moving away from the work surface to prevent contamination. Care was taken to make sure that no volatile chemicals were in the workspace when the Bunsen burner was in use. Sterilization of the inoculation loop and cell spreader was accomplished by placing the tool in the Bunsen burner flame for 10 seconds. The tool was then placed into ethanol at a separate workstation, after which it was placed back into the flame for 5 seconds. Culture tubes and centrifuge tubes used for bacterial cultures were bleached to eliminate bacterial growth. Any pipette tips used were placed into biohazard waste.

A French pressure cell was used to lyse bacterial cells. Operation of the device was always performed in tandem with a graduate student. Due to the weight of the French pressure cell, care was taken to maintain a firm grasp on the device at all times. During operation of the apparatus, one hand continuously grasped the PVC tubing coming from the apparatus to the collection vessel (a Falcon tube). This was performed in case of a large fluctuation in pressure which may cause the tubing to move uncontrollably unless a hand is on the tubing at all times.

Appendix B. Buffers and media.

LB Media (1 L)
- 10 g tryptone
- 5 g yeast extract
- 10 g NaCl
- Add Millipore-distilled H_2O to 1 L
- Autoclave for 15 minutes at 121°C.
- Antibiotic may be added after sterilization.

M9 Media (1L)
- 6.0 g Na_2HPO_4
- 3.0 g KH_2PO_4
- 0.5 g NaCl
- 1.0 mL 40 mg/mL thiamine-HCl (filter sterilized)
- 1.0 mL 1M $MgSO_4$ (autoclaved)
- 10.0 mL trace metals solution
- Add Millipore-distilled H_2O to 1 L
- Filter sterilize solution, then add:
    - 0.5 g NH_4Cl
    - 2.0 g D-glucose

"Buffer A"
- PaGRX: 40 mM Na-Phos, pH 7.0
- BrmGRX, hGRX: 20 mM Tris-Cl pH 8.0
- 200 mM NaCl
- 2 mM dithiothreitol (DTT)
- 20 mM imidazole
- Add Millipore-distilled H_2O to appropriate volume
- Filter, de-gas, store at 4°C.

"Buffer B"
- PaGRX: 40 mM Na-Phos, pH 7.0
- BrmGRX, hGRX: 20 mM Tris-Cl pH 8.0
- 200 mM NaCl
- 2 mM DTT
- 400 mM imidazole
- Add Millipore-distilled H_2O to appropriate volume
- Filter, de-gas, store at 4°C.

Tris-Gly-SDS Electrophoresis Buffer (1 L)
- 30.2 g Tris base
- 188 g glycine (electrophoresis grade)
- 100 mL 10% sodium dodecyl sulfate (SDS; electrophoresis grade)
- Add Millipore-distilled H_2O to 1 L

SDS-PAGE Loading Buffer
- 100 mM Tris-Cl pH 6.8
- 4% (w/v) SDS (electrophoresis grade)
- 0.2% (w/v) bromophenol blue
- 20% (v/v) glycerol
- 200 mM β-mercaptoethanol
- Add Millipore-distilled H_2O to appropriate volume
- Store in freezer.

Blue Silver Colloidal Stain (1 L)
- Add reagents in order listed:
  - 100 mL H_3PO_4 to 100 mL Millipore-distilled H_2O.
  - 100 g $(NH_4)_2SO_4$
  - 1.2 g Coomassie Blue G250
  - Millipore-distilled H_2O to 800 mL total volume.
  - 200 mL EtOH
- Store in dark bottle at room temperature.

Appendix C. Calculated extinction coefficients.

PaGRX
ϵ, 280nm = 15,470 $M^{-1}cm^{-1}$ (6-His tag cleaved)

hGRX
ϵ, 280 nm = 2980 $M^{-1}cm^{-1}$ (6-His tag cleaved)

BrmGRX
ϵ, 280 nm = 4470 $M^{-1}cm^{-1}$ (6-His tag cleaved)

coumarin acrylamide
ϵ, 328 nm = 10,717 $M^{-1} cm^{-1}$